Stiffness and Conformational Transition of Poly{3-[(*S*)-2-methylbutoxy]phenyl isocyanate} in Dilute Solution

Kazuto Yoshiba,*,† Ryota Hama, Akio Teramoto,* and Naotake Nakamura

Research Organization of Science and Engineering, Ritsumeikan University, Noji-higashi 1-1-1, Kusatsu, Siga 525-8577, Japan

Katsuhiro Maeda and Yoshio Okamoto

Department of Applied Chemistry, Graduate School of Engineering, Nagoya University, Furo-cho, Chikusa-ku, Nagoya 464-01, Japan

Takahiro Sato

Department of Macromolecular Science, Osaka University, Machkaneyama-cho 1-1, Toyonaka, Osaka 560-0022, Japan

Received January 12, 2006; Revised Manuscript Received February 28, 2006

ABSTRACT: Poly{3-[(*S*)-2-methylbutoxy]phenyl isocyanate} was shown to be locally helical, but a rather flexible wormlike chain of persistence length 3 nm. Its optical activity changed remarkably on temperature−solvent and molecular weight, vanishing at a specific temperature T_c irrespective of molecular weight, exhibiting a cooperative transition of helical conformations. Such optical activity data were well explained by a theory of Lifson et al. on the helix reversal model, taking the conformations of the terminal residues explicitly. This polymer is locally helical and rodlike because of its conjugating main-chain amide bonds, which are conjugating also with side-chain phenyl rings. However, the latter conjugation weakens the main-chain stiffness, with almost no contribution to the global stiffness from helix reversal points.

1. Introduction

Polyisocyanates are known to be typical semiflexible polymers,[1−4] and those with chiral pendent groups exhibit large optical activity, e.g., molar ellipticity $[\theta]$.[5] This is because the amide groups of partial double-bond character constituting the main chain tend to be trans-planar, resulting in a rodlike conformation, but it is difficult to become so because of interactions of side groups with the main chain.[6] To avoid this difficulty, the main chain makes an internal rotation slightly off the trans-planar position, resulting in a helical conformation.

When there is some chiral perturbation, particularly with a chiral side chain, one of the left-handed and right-handed helices is favored over the other, and the polymer shows net optical activity, which is largely enhanced on the polymer chain. Green and collaborators found this is indeed the case with stereospecifically deutrated poly(hexyl isocyanate)s.[5,7,8] The optical activity changed with polymer molecular weight and temperature, and this change was analyzed by Lifson et al.[8] on the helix reversal model. The conformational transitions of these polymers[9,10] were studied in detail and analyzed successfully by Lifson's theory. Later similar transitions were found with achiral polyisocyanates with chiral initiators,[11,12] copolyisocyanantes,[13] and chiral polysilylenes.[14−17] The good agreement between experiment and theory[8−10,13,15,16,18,19] is expected to clarify the molecular mechanism behind this transition that in a polymer chain left-handed and right-handed helical sections coexist, which are connected alternatively via helix reversal points, and the net helicity is determined by the free energy balance between the two helical conformations and the transition probability across the helix reversal.

In most cases $[\theta]$ changes with temperature but does not change its sign. However, there are some exceptions,[16,20−23] where it changes the sign at a critical temperature T_c. The transition of one of such polysilylenes, poly{[(*R*)-3,7-dimethyloctyl]-[(*S*)-3- methylpentyl]silylene} (PRS),[16] was studied in detail to find that T_c is independent of molecular weight. Theoretically, the *N*-independent T_c results from the lack of a conformational restriction on the terminal residues such that they can be involved in either left-handed or right-handed helical conformation. Recently Maeda et al.[20−22] synthesized polyisocyanates bearing an optically active phenyl ring, and some of them exhibited thermal transition of helix sense reversal. The purpose of the present study is to confirm whether this is a phenomenon specific to this system or a general predicted by the general theory proposed previously choosing one of such polymers, poly{3-[(*S*)-2-methylbutoxy]phenyl isocyanate} (P3(*S*)2MBuOPI).[22,24] The stiffness of this polymer is of another interest because it is suggested that a polyisocyanate with a phenyl group attached directly to the amide group might be flexible.

2. Experimental Section

Polymer Samples and Solutions. Original poly{3-[(*S*)-2-methylbutoxy]phenyl isocyanate} samples of different molecular weights were obtained by polymerizing 3-[(*S*)-2-methylbutoxy]phenyl isocyanate with lithium amide as an initiator.[24] About 1 g of them was separated into many fractions of different molecular weights by gel permeation chromatography (GPC) with two Shodex 2006M columns connected in series on toluene solutions at 40 °C. The fractionated samples were freeze-dried from benzene solutions to obtain six samples designated as KP-1, KP-2, ..., KP-6. Every solution used in the following measurements was prepared by dissolving a weighed amount of each sample in distilled terahydrofuran (THF) or dichloromethane (DCM). The polymer mass concentration *c* of each solution was determined gravimetrically

† Present address: Department of Biological and Chemical Engineering, Faculty of Engineering, Gumma University, 1-5-1, Tenjin-cho, Kiryu, Gumma 355-8515, Japan.

10.1021/ma060083p CCC: $33.50
Published on Web 04/08/2006

Table 1. Molecular Characterization of P3(*S*)2MBuOPI Samples in THF at 25 °C

code	M_w/1000	M_z/M_w	10^4A_2/cm^3 mol g^{-2}	$\langle S^2\rangle_z^{1/2}$/nm	$[\eta]$/cm^3 g^{-1}	k'
KP-1	300[b]	1.1$_0$[c]	3.1[b]	20[b]	71.8	0.38
KP-2	175[b]	1.1$_2$[c]	3.3[b]	14[b]	49.6	0.38
KP-3	100[b]	1.0$_9$[c]	4.3[b]		30.5	0.39
KP-4	66.2[a]	1.1$_0$[a,c]	5.6[a]		20.5	0.48
KP-5	42.4[b]	1.1$_0$[c]	5.5[b]		16.9	0.44
KP-6	24.3[a]	1.1$_3$[a,c]	5.3[a]		12.2	0.49

[a] Sedimentation equilibrium. [b] Light scattering. [c] GPC.

using the necessary densities ρ at temperature T of DCM and THF: $1/\rho = 0.001025(T/°C) + 0.7340$ and $1/\rho = 0.001194 \times (T/°C) + 1.1064$, respectively.

Light Scattering and Sedimentation Measurements. Light scattering measurements were made on a Wyatt Technology DAWN DSP multiangle light scattering photometer for samples KP-1, KP-2, KP-3, and KP-5, and sedimentation equilibrium measurements were made a Beckman OPTIMA-XL-I ultracentrifuge with Rayleigh interference optics for KP-4 and KP-6 with THF as the solvent. Densities of THF solutions were determined by using an Anton Paar DMA 5000 densitometer, and the partial specific volume v of P3(*S*)2MBuOPI at 25 °C was found to be 0.876 cm^3 g^{-1}. The specific refractive index increment $\partial n/\partial c$ at the wavelength 633 nm was determined by using a Wyatt Technology POTILAB DSP to be 0.138 cm^3 g^{-1}. The polydispersity index M_z/M_w was determined from either sedimentation equilibrium or GPC measurements with TSKgel G5000H$_{HR}$ and G2500H$_{HR}$ columns connected in series using a calibration curve constructed from the retention times and M_w values measured.

Viscosity and Spectroscopic Measurements. Viscosities of THF solutions of the six samples were measured at 25 °C with an Ubbelohde capillary viscometer to determine their intrinsic viscosities $[\eta]$ and Huggins' constants k'. Circular dichroism (CD) and absorption (UV) spectra of THF and DCM solutions were measured on a JASCO J-720 spectropolarimeter at temperatures between −65 and 30 °C. The temperature of the solution was controlled by a cryostat, whose temperature was calibrated by a thermocouple put in the solution cell.

3. Results

Molecular Characteristics and Viscosity Behavior. Light scattering and sedimentation equilibrium data were analyzed following the established procedures,[25] yielding the results summarized in Table 1. The six samples range in M_w between 24 300 and 300 000 and are reasonably narrow in molecular-weight distribution as judged from the M_z/M_w values determined. It also contains values of intrinsic viscosity $[\eta]$ and Huggins coefficient k'. As seen from the second virial coefficient values A_2 and k', THF is a rather good solvent for this polymer. The z-average radius of gyration $\langle S^2\rangle_z^{1/2}$ has been determined only for the two largest molecular weight samples because it was too small with the other samples. It is noted that $[\eta]$ is much small for this polymer and depends considerably less on molecular weight compared with those for poly(alkyl isocyanate)s.[1−4] This point will be discussed below in more detail in terms of persistence length q. The weight-average degree of polymerization N_w was calculated by $N_w = M_w/205.3$.

UV and CD Spectra. Figure 1 shows UV and CD spectra of KP-1 and KP-6 (highest and lowest molecular weight samples) at 10 °C and of KP-1 at −53 °C in THF, where ϵ and $[\theta]$ are the monomer unit molar extinction coefficient and ellipticity, respectively, and λ is the wavelength. It is seen that the UV spectrum is essentially the same for the two samples and also so at the two temperatures. On the other hand, the height and sign of the CD spectrum are seen to change with sample and temperature, respectively, but each looks very similar in shape with a big peak around 270 nm. To be more precise, this peak consists of two peaks: the main one around 270 nm and the other at higher wavelengths as a shoulder. However, it is shown that all the spectra are reduced to a single composite one when adjusted at a fixed main peak height. Therefore, the height of the main peak, $[\theta]_{270}$, at 270 nm can be taken as a measure for the net optical activity.

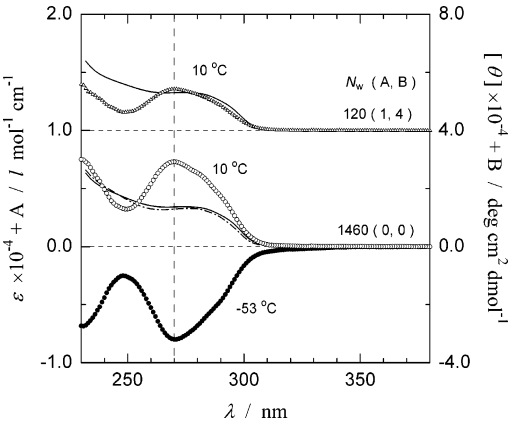

Figure 1. CD $[\theta]$ and UV ϵ spectra of KP-1 at 10 °C (unfilled circles and solid curve, respectively) and −53 °C (filled circles and dot−dashed curve) and of KP-6 at 10 °C (unfilled triangles and solid curve) in THF. The spectra are shifted vertically by the values in the parentheses: A for ϵ and B for $[\theta]$.

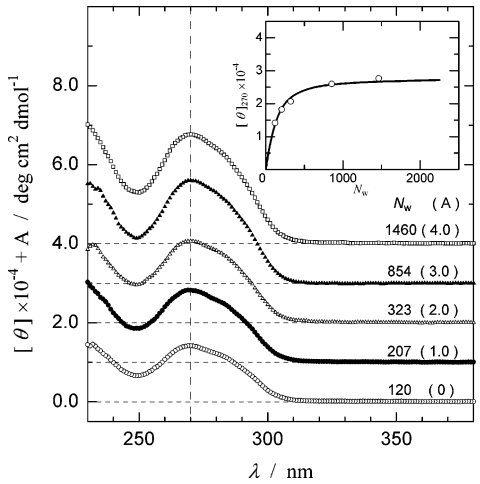

Figure 2. CD spectra of five P3(*S*)2MBuOPI samples at 25 °C in THF. The spectra are shifted vertically by the values in the parentheses. The inset is the N_w dependence of the molar ellipticity $[\theta]_{270}$ at the maximum wavelength of 270 nm at 25 °C.

CD spectra of samples with different N_w are shown in Figure 2, where each curve is shifted upward by A in parentheses for clarity. Here again each curve has the same shape, but the magnitude of $[\theta]$ is bigger for larger N_w. The N_w dependence of $[\theta]_{270}$ is more explicitly illustrated in the inset. It is seen that $[\theta]_{270}$ increases rapidly with N_w at lower N_w but tends to level off above N_w of 1000. This is indeed a typical trend in linear cooperative systems, which undergoes a thermal transition, as also found with chiral polyisocyanates[7−10] and polysilylenes.[14−17]

Figure 3 shows the temperature dependence of $[\theta]_{270}$ for samples with different N_w. For each sample the value of $[\theta]_{270}$ changes from negative to positive as the temperature T is raised, exhibiting a thermal transition. The transition is more conspicuous for larger N_w, but all the curves cross zero around T_c of −32 °C.

Similar $[\theta]_{270}$ data for P3(*S*)2MBuOPI in DCM are given in Figure 4. Here again $[\theta]_{270}$ changes with temperature and

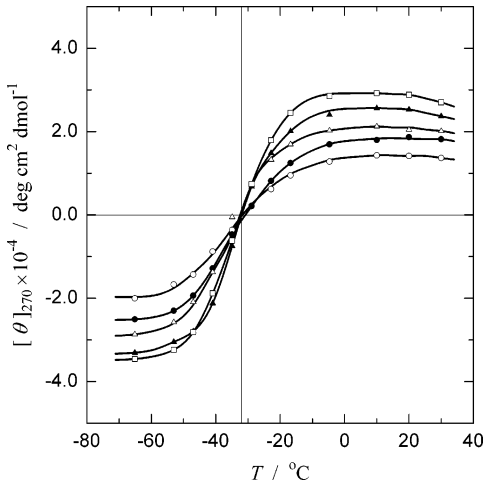

Figure 3. Temperature dependence of $[\theta]_{270}$ of P3(*S*)2MBuOPI samples in THF. Symbols: unfilled circles, KP-6; filled circles, KP-5; unfilled triangles, KP-4; filled triangles, KP-2; unfilled squares, KP-1; solid curves, guides for the eye.

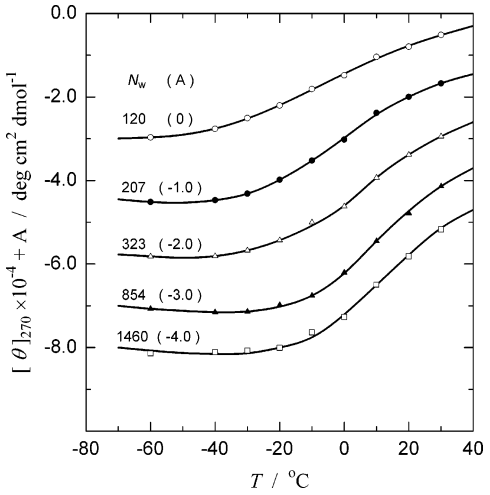

Figure 4. Temperature dependence of $[\theta]_{270}$ of P3(*S*)2MBuOPI samples in dichloromethane. The data points are shifted vertically by the values in the parentheses; the same symbols are used as those in Figure 3. Solid curves are guides for the eye.

molecular weight, which is common to linear cooperative transitions. However, no T_c is found in this temperature range similarly to the transition in stereospecifically deuterated poly(hexyl isocyanate)s.[9,10] Figure 5 shows the CD spectra of the P3(*S*)2MBuOPI samples in the mixed solvents of THF and DCM in order to investigate the T_c variance; the inset represents the temperature dependence of the $[\theta]_{270}$ labeled by mole ratio of their solvent compositions. The spectra showed the same feature of the system of the single solvent; i.e., the peak of each spectrum is located at 270 nm, and the peak strength depends extremely on the temperature, which passes through the $[\theta]_{270} = 0$ at the reversal point T_c. The increase in DCM content makes the strength at 270 nm smaller and T_c shifted to higher temperatures, although both spectra of CD and UV remain the same shapes over all the compositions and temperatures.

The thermally induced helix sense reversal is the behavior found previously in poly{[(*R*)-3,7- dimethyloctyl]-[(*S*)-3-methylpentyl]silylene} (PRS),[16] and thus the existence of critical temperature T_c is the general feature common to some group of linear cooperative systems on specific solvent conditions. The optical activity due to chiral side chain is largely amplified on this polymer chain. It is clear that this large optical activity originates from the unbalance in helical conformations, which

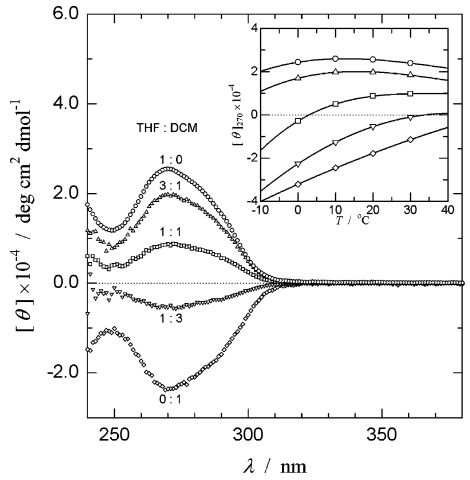

Figure 5. CD spectra of KP-2 in mixed solvents of THF and dichloromethane (DCM) at 20 °C. The compositions of the solvents are represented by the weight ratio of THF to DCM. The inset is the temperature dependence of $[\theta]_{270}$ in mixed solvents. The same symbols are used in the main figure and inset.

undergoes a transition from the left-handed to right-handed helices, and vice versa. Tang et al.[23] also reported similar solvent−temperature behavior for copolyisocyanates, where T_c can be controlled by the copolymer composition.

Lifson et al.[6] showed by an effective force field calculation that the negative CD band around 270 nm may be attributed to a left-handed helix for the main chain of polyiocyanate. Therefore, the temperature dependence of $[\theta]_{270}$ indicates that the dominant helix sense changes from left-handed to right-handed as T is raised from −65 to 30 °C; T_c can be located at −32 °C. The reversal of helix sense of this type has been found recently in other polymers, namely polysilylenes[17] and copolyisocyanates.[23]

4. Discussion

Theoretical Analysis of CD Data. The main chain of P3(*S*)2MBuOPI tends to be coplanar, but because of the interaction between side chains, it is distorted to form helical conformations. However, the same helical conformation does not persist over the whole length, but right-handed and left-handed helices coexist on the same chain. This is the helix reversal model of Lifson et al.[8] It is formulated in a more general way taking the state of terminal residues as follows.[18,19] The partition function Z_N of such a chain is represented by

$$Z_N = \mathbf{A}\mathbf{M}^{N-1}\mathbf{B} \tag{1}$$

with **M** being the statistical weight matrix defined by

$$M = \begin{pmatrix} u_M & \upsilon u_P \\ \upsilon u_M & u_P \end{pmatrix} \tag{2}$$

where u_M is the statistical weight of the M residue, u_P is that for the P residue, and υ is the transition probability from M to P or P to M. The ratio u_M/u_P is related to their free energies as $u_M/u_P = \exp(-2\Delta G_h/RT)$, where $2\Delta G_h = G_M - G_P$ is the free energy difference between the two residues and υ is related to the helix reversal energy ΔG_r by $\upsilon = \exp(-\Delta G_r/RT)$. The vectors **A** and **B** are defined to specify the situations of the terminal residues by

$$\mathbf{A} = (au_M \;\; u_P) \qquad \mathbf{B} = (b \;\; 1) \tag{3}$$

such that they take any conformation when $a = b = 1$, and

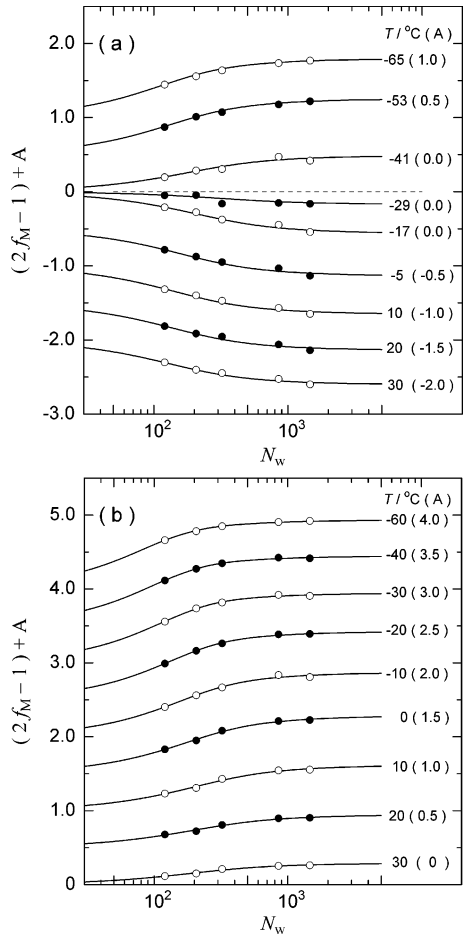

Figure 6. N_w dependence of $2f_M - 1$ in (a) THF and (b) dichloromethane solutions at different temperatures. Curves: theoretical values of the fraction f_M of the M-helix with the assumed value of $[\theta]_M = -4.3 \times 10^4$ for the left-handed perfect helix and with the optimal values of ΔG_h and ΔG_r; $a = b = 1$.

they cannot take M conformation when they are zero. The fraction of M-helix, f_M, can be derived from Z_N by the standard statistical procedure.

The helix−coil transition in polypeptide and order−disorder transition in aqueous schizophyllan correspond to the latter case, whereas the former is the case with polyisocyanates and polysilylenes. Therefore, if the experimental dependence of $[\theta]_{270}$ at a fixed solvent condition follows the theoretical values with appropriate parameter values for u_M/u_P and υ, the theoretical consideration is justified, and the parameter values are obtained as functions of solvent condition. This allows one to discuss the optical activity concerned on a molecular level.

To test this theoretical prediction, it is necessary to convert $[\theta]_{270}$ to f_M. In conformity with Lifson's calculation,[6] we let M be left-handed and P right-handed and take the value of $[\theta]_{270}$ for a perfect left-handed helix $[\theta]_M$ to be $-43\,000$ deg cm^2 dmol^{-1} [34] with u_M/u_P and υ or $2\Delta G_h$ and ΔG_r as adjustable parameters; $f_M = (1/2)([\theta]_{270}/[\theta]_M - 1)$. Figure 6a shows plots of $2f_M - 1$ against N_w in THF at fixed temperatures. At each temperature the data points are fitted precisely by the solid curve, which represents the theoretical values calculated with appropriate values for $2\Delta G_h$ and ΔG_r and $a = b = 1$. Figure 6b illustrates the result from a similar analysis of the DCM solution data with $a = b = 1$. The fitting is reasonably good for all the samples at all temperatures studied.

Figure 7 compares the values of $2\Delta G_h/RT$ and $\Delta G_r/RT$ obtained for our systems with those for other systems, where

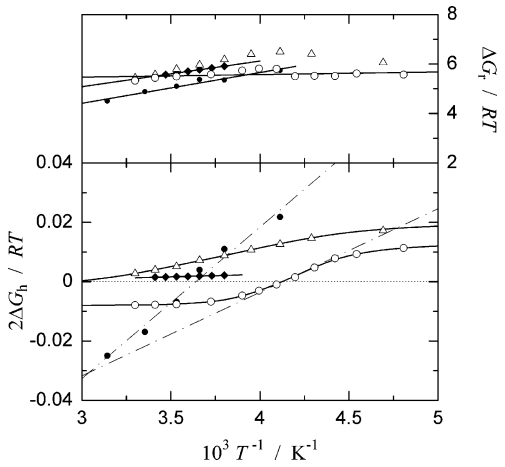

Figure 7. Temperature dependence of the free energy differences between the left- and right-handed helix $2\Delta G_h$ and the helix reversal free energy ΔG_r for P3(*S*)2MBuOPI in THF (unifilled circles) and DCM (unfilled triangles), PRS in isooctane (filled circles),[16] and a stereospecifically duterated poly(*n*-hexyl isocyanate) in dichloromethane (filled diamonds).[9] The reversal temperature is −32 °C for P3(*S*)2MBuOPI in THF and 3 °C for PRS in isooctane. The solid curves are guides for the eye.

unfilled circles represent those for P3(*S*)2MBuOPI in THF and filled circles those for PRS in isooctane;[16] both exhibit helix sense reversal. Indeed, in the two systems $2\Delta G_h/RT$ changes with T similarly and becomes zero at T_c. However, the change is larger for PRS than for the present polymer. On the other hand, $\Delta G_r/RT$ for this polymer stays essentially constant in the temperature range examined, whereas that for PRS increases significantly with $1/T$. These differences may be ascribed to the large side-chain groups on PRS, which induce larger structural asymmetry between left-handed and right-handed helical conformations of PRS. The magnitude of $2\Delta G_h/RT$ is much larger for P3(*S*)2MBuOPI than for chirally deuterated PHIC (filled diamonds).[9,10] This is obviously due to the smaller chiral group, deuterium D, on the latter. However, the opposite is the case with $\Delta G_r/RT$, which dictates the probability of crossing the reversal point, which is small for polyisocyanates because it requires a cis−trans conformational transition of high energy in the amide bond.[6] These parameter values tell one that the main chain of P3(*S*)2MBuOPI consists of an alternating sequence of left-handed and right-handed helical chains of relatively short persistence in THF. To be precise, the persistence at low temperatures appears longer in DCM than in THF. However, they (three points) may be outside the uncertainty in persistence in DCM.

The free energy difference $2\Delta G_h$ is related to the internal rotation energy $E(\tilde{\phi})$ of the main-chain bond rotation angle $\tilde{\phi}$. In the vicinity of the stable left-handed (M) or right-handed (P) helical states specified by $\tilde{\phi} = \tilde{\phi}_M$ and $\tilde{\phi}_P$, $E(\tilde{\phi})$ is approximately written as $E(\tilde{\phi}) = E_X + a_X(\tilde{\phi} - \tilde{\phi}_X)^2$ (X = M or P), where E_X and a_X are respectively the minimum energy and the force constant in the M or P state. Using the relation between $2\Delta G_h$ and $E(\tilde{\phi})$, we have

$$2\Delta G_h = \Delta H_h - T\Delta S_h \tag{4}$$

with the enthalpy component $\Delta H_h = E_M - E_P$ and entropy component $\Delta S_h = (R/2)\ln(a_P/a_M)$. If $E(\tilde{\phi})$ is independent of T, ΔH_h and ΔS_h are temperature independent, and $2\Delta G_h/RT$ is linearly dependent on T^{-1}. This is the case for PRS as shown in Figure 7. On the other hand, $2\Delta G_h/RT$ for P3(*S*)2MBuOPI in THF exhibits a sigmoidal temperature dependence. This may

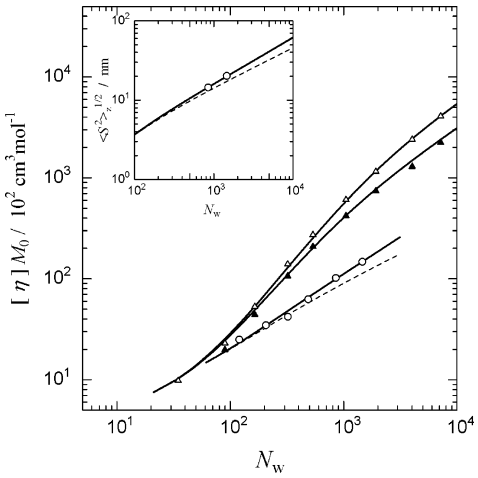

Figure 8. N_w dependence of $[\eta]$ multiplied by the molar mass M_0 of the monomer unit for P3(S)2MBuOPI in 25 °C THF (unfilled circles), PHIC in 25 °C toluene (unfilled triangles), and PHIC in 20 °C dichloromethane (filled triangles). Thick and thin solid curves indicate theoretical values calculated by the theory for perturbed wormlike touched-bead model with the model parameters (M_L, d_B, q, B) equal to (1194 nm^{-1}, 2.1 nm, 3 nm, 2 nm) for P3(S)2MBuOPI in THF, (740 nm^{-1}, 1.9 nm, 37 nm, 0) for PHIC in toluene, and (740 nm^{-1}, 1.9 nm, 21 nm, 0) for PHIC in dichloromethane. The inset compares the radius gyrations of P3(S)2MBuOPI fractions of KP-1 and KP-2 in THF with the Benoit−Doty theory for the wormlike chain model with $M_L = 1082$ nm^{-1}, $q = 3.3$ nm, and $B = 1.7$ nm. Dashed curves in both figures are the unperturbed chain calculated with $B = 0$.

be due to a temperature dependence of $E(\tilde{\phi})$ itself for this helical polymer.

It has been shown that the theoretical framework for linear cooperative transitions considering the state of the end residues expressed by the two parameters, a and b, is of general applicability.[19] So far, we have proved this applicability on the systems of helix−coil in polypeptides ($a = b = 0$),[31,32] order−disorder transition in aqueous schizophyllan ($a = b = 0$),[19] helix reversal in polyisocyanates and polysilylenes ($a = b = 1$), and achiral polyisocyanates polymerized with chiral initiator ($a = 1$, $b = 0$),[18,20−22] in addition to P3(*S*)2MBuOPI ($a = b = 1$).

Stiffness of P3(*S*)2MBuOPI in THF. In Figure 8, the $[\eta]$ vs N_w dependence of P3(*S*)2MBuOPI in THF at 25 °C (circles) is compared with those of poly(*n*-hexyl isocyanate) (PHIC) in two solvents (triangles), where the $[\eta]$ data are reduced by multiplying the monomer molecular weight M_0. PHIC is known to be a typical semiflexible polymer; q is 37 and 21 nm respectively in toluene and DCM.[4] It is obvious that the present polymer is much less stiff than PHIC from its lower $[\eta]$ values less dependent on N_w.

It is usual to estimate the stiffness of a polymer chain in terms of the wormlike touched-bead model,[26] where the stiffness is expressed by the persistence length q, which is a measure how close the chain conformation to a rigid rod. This model is characterized by the mass per unit length M_L, the bead diameter d_B, and q;[26] the molecular weight M is related to the contour length L by $L = M/M_L$. For a flexible polymer the excluded-volume effect must be considered to describe the chain conformation precisely, introducing the excluded-volume parameter B.[26,27]

An analysis of $[\eta]$ vs N_w relation tests this theory to derive the values for the involved model parameters. However, the present viscosity data for this polymer are not detailed enough to allow such an analysis. It has been found that M_L and d_B may be evaluated in good approximation from the chemical structure and partial specific volume.[3] Therefore, we used

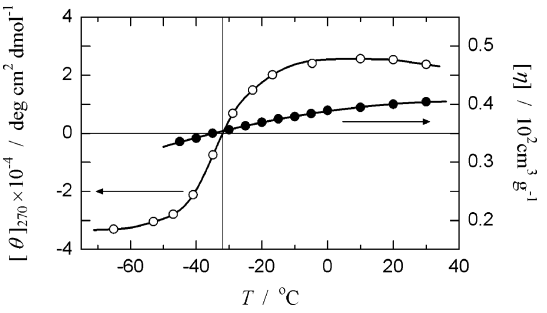

Figure 9. Temperature dependence of $[\eta]$ and $[\theta]_{270}$ for a P3(S)2MBuOPI sample with the weight-average molecular weight $M_w = 13.2 \times 10^4$ in THF over the range of temperature encompassing T_c. Solid curves are guides for the eye.

appropriate values for these parameters ($M_L = 1194$ nm^{-1}, $d_B = 2.1$ nm) and kept q and B as adjustable parameters. Fitting the data to the theory on this condition gave values of q and B, which are correlated one another such that the larger q smaller B, although it was impossible to have a reasonable fit with $B = 0$. Thus, we conclude that their optimal values are $q = 3$ nm and $B = 2$ nm within 1 nm. The theoretical solid curve with these values (the thick solid curve in Figure 8) follows the data points precisely; the dashed curve in the figure represents the unperturbed values of $[\eta]$, and the excluded-volume effect is small but discernible. As seen in the insert, $\langle S^2\rangle_z^{1/2}$ data of P3(*S*)2MBuOPI in THF at 25 °C are also consistently described by the Benoit−Doty theory[33] for the wormlike chain model with almost the same parameter set of M_L, q, and B. Thus, we see this polymer is rather flexible compared with most semiflexible polymers, but evidently stiffer than polystyrene, which is a typical flexible polymer of q around 1 nm.[3]

Figure 9 shows the temperature dependence of $[\eta]$ for a P3(*S*)2MBuOPI sample in THF over the range of temperature encompassing T_c where $[\theta]_{270}$ changes its sign. It is noted that $[\eta]$ increases gradually with T even in the inversion region of $[\theta]_{270}$; thus, $[\eta]$ undergoes no transition at T_c. A similar T insensitivity of $[\eta]$ in the transition region has been found for poly{[(*R*)-3,7-dimethyloctyl]-[(*S*)-3-methylpentyl]silylene} (PRS).[16] The present polymer is the first example showing both thermally and solvent induced helix sense inversions, indicating that both structure of the polymer and interactions with solvent are important for the transition.

As mentioned previously,[29,30] helical polymer chains with helix reversals are more suitably modeled by the broken wormlike chain[28] of which effective persistence length q is written as

$$\frac{1}{q} = \frac{f_M}{q_{0,M}} + \frac{1 - f_M}{q_{0,P}} + \frac{1 - \cos\hat{\theta}_V}{\langle l\rangle} \qquad (5)$$

where $q_{0,X}$ (X = M or P) is the persistence length of each helical segment, $\hat{\theta}_V$ is the angle at the kink, and $\langle l\rangle$ is the arithmetic mean length of M and P helices. The intrinsic persistence length $q_{0,X}$ is related to $E(\tilde{\phi})$, the internal rotation energy of the main-chain amide bond rotation $\tilde{\phi}$.

From the results of ΔG_r and ΔG_h determined above, it turns out that $\langle l\rangle$ in eq 5 is much larger than the total q for P3(*S*)2MBuOPI, and the small q must come from small $q_{0,i}$. Thus, the flexibility of this polymer mostly arises from large fluctuation in the internal rotation of the main chain, or shallow minima of $E(\tilde{\phi})$, maybe because the pendent phenyl rings directly attached to the main chain amide groups weaken conjugation within the main chain.

If $E(\tilde{\phi})$ is independent of temperature, fluctuation in the internal rotation of the main chain should increase, so that q must decrease, with increasing temperature. Usually q for helical polymers exhibits this normal temperature dependence,[29,30] but Figure 9 shows a positive temperature dependence of $[\eta]$ for P3(*S*)2MBuOPI in THF. Since THF is a good solvent for this polymer where the excluded-volume effect is insensitive to temperature, this dependence of $[\eta]$ should mainly reflect the positive temperature dependence of q. This may be due to a temperature dependence of $E(\tilde{\phi})$ for this helical polymer as already mentioned in the relation with the sigmoidal temperature dependence of $2\Delta G_h/RT$. If the fluctuation of the bulky side chain conformation increases with temperature, the available internal rotation angle of the main chain may be more restricted, so that the minima of $E(\tilde{\phi})$ may become steeper with increasing temperature, which can increase $q_{0,X}$ or q.

Acknowledgment. A.T. thanks Dr. Hachiro Kawamoto, Chancellor of Ritsumeikan University, for the Chair-Professorship at Ritsumeikan University.

Supporting Information Available: Detailed data of $[\theta]$. This material is available free of charge via the Internet at http://pubs.acs.org.

References and Notes

(1) Murakami, H.; Norisuye, T.; Fujita, H. *Macromolecules* **1980**, *13*, 345−352.
(2) Kuwata, M.; Murakami, H.; Norisuye, T.; Fujita, H. *Macromolecules* **1984**, *17*, 2731−2734.
(3) Norisuye, T. *Prog. Polym. Sci.* **1993**, *18*, 543−584.
(4) Itou, T.; Chikiri, H.; Teramoto, A. *Polym. J.* **1996**, *28*, 357−361.
(5) Green, M. M.; Andreola, C.; Munos, B.; Reidy, M. P. *J. Am. Chem. Soc.* **1988**, *110*, 4063−4064.
(6) Lifson, S.; Felder, C. E.; Green, M. M. *Macromolecules* **1992**, *25*, 4142−4148.
(7) Green, M. M.; Peterson, N. C.; Sato, T.; Teramoto, A.; Cook, R.; Lifson, S. *Science* **1995**, *268*, 1860−1866.
(8) Lifson, S.; Andreola, C.; Peterson, N. C.; Green, M. M. *J. Am. Chem. Soc.* **1989**, *111*, 8850−8858.
(9) Gu, H.; Nakamura, Y.; Sato, T.; Teramoto, A.; Green, M. M.; Andreola, C.; Peterson, N. C.; Lifson, S. *Macromolecules* **1995**, *28*, 1016−1024.
(10) Okamoto, N.; Mukaida, F.; Gu, H.; Nakamura, Y.; Sato, T.; Teramoto, A.; Green, M. M.; Andreola, C.; Peterson, N. C.; Lifson, S. *Macromolecules* **1996**, *29*, 2878−2884.
(11) Okamoto, Y.; Matsuda, M.; Nakano, T.; Yashima, E. *Polym. J.* **1993**, *25*, 391.
(12) Maeda, K.; Matsuda, M.; Nakano, T.; Yashima, E. *Polym. J.* **1995**, *27*, 141.
(13) Gu, H.; Nakamura, Y.; Sato, T.; Teramoto, A.; Green, M. M.; Jha, S. K.; Reidy, M. P. *Macromolecules* **1998**, *31*, 6362−6368.
(14) Fujiki, M. *J. Am. Chem. Soc.* **2000**, *122*, 3336−3343. (b) Fujiki, M.; Koe, J. R.; Nakashima, H.; Motonaga, M. Terao, K.; Teramoto, A. *J. Am. Chem. Soc.* **2001**, *123*, 6253−6261.
(15) Terao, K.; Terao, Y.; Teramoto, A.; Nakamura, N.; Fujiki, M.; Sato, T. *Macromolecules* **2001**, *34*, 6519−6525.
(16) Teramoto, A.; Terao, K.; Terao, Y.; Terao, Y.; Nakamura, N.; Sato, T.; Fujiki, M. *J. Am. Chem. Soc.* **2001**, *123*, 12303−12310.
(17) Fujiki, M.; Koe, J. R.; Terao, K.; Sato, T.; Teramoto, A.; Watanabe, J. *Polym. J.* **2003**, *35*, 297−344.
(18) Gu, H.; Sato, T.; Teramoto, A.; Varichon, L.; Green, M. M. *Polym. J.* **1997**, *29*, 77−84. Sato, T.; Terao, K.; Teramoto, A.; Fujiki, M. *Macromolecules* **2002**, *35*, 5355−5357.
(19) Teramoto, A. *Prog. Polym. Sci.* **2001**, *26*, 667−720.
(20) Maeda, K.; Okamoto, Y. *Macromolecules* **1998**, *31*, 5164−5166.
(21) Maeda, K.; Okamoto, Y. *Macromolecules* **1999**, *32*, 974−980.
(22) Hino, K.; Maeda, K.; Okamoto, Y. *J. Phys. Org. Chem.* **2000**, *13*, 361−367.
(23) Tang, K.; Green, M. M.; Cheon, K. S.; Selinger, J. V.; Garetz, B. A. *J. Am. Chem. Soc.* **2003**,*125*, 7031.
(24) Hino, K. MS Thesis, Nagoya University, 1999.
(25) Terao, K.; Terao, Y.; Teramoto, A.; Nakamura, N.; Terakawa, I.; Fujiki, M.; Sato, T. *Macromolecules* **2001**, *34*, 4519−4525.
(26) Yamakawa, H. *Helical Wormlike Chains in Polymer Solutions*; Springer: Berlin, 1997.
(27) Norisuye, T.; Tsuboi, S.; Teramoto, A. *Polym. J.* **1988**, *20*, 143−151.
(28) Mansfield, M. L. *Macromolecules* **1986**, *19*, 845−859.
(29) Sato, T.; Terao, K.; Teramoto, A. Fujiki, M. *Macromolecules* **2002**, *35*, 2141−2148.
(30) Sato, T.; Terao, K.; Teramoto, A.; Fujiki, M. *Polymer* **2003**, *44*, 5477−5495.
(31) Teramoto, A.; Fujita, H. *Adv. Polym. Sci.* **1975**, *18*, 65−149.
(32) Teramoto, A.; Fujita, H. *J. Macromol. Sci., Rev. Macromol. Chem.* **1976**, *C15*, 165−278.
(33) Benoit, H.; Doty, P. *J. Chem. Phys.* **1953**, *57*, 958.
(34) Plots of $[\theta]_{270}$ vs $1/N_w$ in DCM at −40 and −60 °C were used to determine the values of $[\theta]_M$ for the perfect M-helix. The same values were used for both DCM and THF data.

MA060083P